

SDSS J1335+0118: A New Two-Image Gravitational Lens

Masamune OGURI,¹ Naohisa INADA,¹ Francisco J. CASTANDER,² Michael D. GREGG,^{3,4}
Robert H. BECKER,^{3,4} Shin-Ichi ICHIKAWA,⁵ Bartosz PINDOR,⁶ Jonathan BRINKMANN,⁷
Daniel J. EISENSTEIN,⁸ Joshua A. FRIEMAN,^{9,10} Patrick B. HALL,⁶ David E. JOHNSTON,⁹
Gordon T. RICHARDS,⁶ Paul L. SCHECHTER,¹¹ Donald P. SCHNEIDER,¹² and Alexander S. SZALAY¹³

¹*Department of Physics, University of Tokyo, Hongo 7-3-1, Bunkyo-ku, Tokyo 113-0033.*

²*Institut d'Estudis Espacials de Catalunya/CSIC, Gran Capita 2-4, 08034 Barcelona, Spain.*

³*Department of Physics, University of California at Davis,
1 Shields Avenue, Davis, CA 95616, USA.*

⁴*Institute of Geophysics and Planetary Physics, Lawrence Livermore National Laboratory,
L-413, 7000 East Avenue, Livermore, CA 94550, USA.*

⁵*National Astronomical Observatory, 2-21-1 Osawa, Mitaka, Tokyo 181-8588.*

⁶*Princeton University Observatory, Peyton Hall, Princeton, NJ 08544, USA.*

⁷*Apache Point Observatory, P.O. Box 59, Sunspot, NM88349, USA.*

⁸*Steward Observatory, University of Arizona,
933 North Cherry Avenue, Tucson, AZ 85721, USA.*

⁹*Astronomy and Astrophysics Department, University of Chicago,
5640 South Ellis Avenue, Chicago, IL 60637, USA.*

¹⁰*Fermi National Accelerator Laboratory, P.O. Box 500, Batavia, IL 60510, USA.*

¹¹*Department of Physics, Massachusetts Institute of Technology,
77 Massachusetts Avenue, Cambridge, MA 02139, USA.*

¹²*Department of Astronomy and Astrophysics, Pennsylvania State University,
525 Davey Laboratory, University Park, PA 16802.*

¹³*Department of Physics and Astronomy, Johns Hopkins University,
3701, San Martin Drive, Baltimore, MD 21218, USA.*

(Received ; accepted)

Abstract

We report the discovery of the two-image gravitationally lensed quasar SDSS J1335+0118. The object was selected as a lens candidate from the Sloan Digital Sky Survey. The imaging and spectroscopic follow-up observations confirm that the system exhibits two gravitationally lensed images of a quasar at $z = 1.57$. The image separation is $1''.56$. We also detect an extended component between the two quasar images, likely the lensing galaxy. Preliminary mass modeling predicts the differential time delay $\Delta t \sim 30h^{-1}\text{day}$ assuming the redshift of the lens galaxy is 0.5.

Key words: gravitational lensing — quasars: individual (SDSS J133534.79+011805.5)

1. Introduction

Multiple images of a quasar produced by a foreground galaxy are useful for cosmological and astrophysical applications, including the measurement of the cosmological constant through the lensing rate (Turner 1990; Fukugita, Futamase, & Kasai 1990; Chae et al. 2002), the determination of global Hubble constant from time delays between images (Refsdal 1964, 1966), the study of the mass distributions of the lensing galaxies (Kochanek 1991; Metcalf & Madau 2001; Chiba 2002; Dalal & Kochanek 2002; Schechter & Wambsganss 2002; Koopmans & Treu 2003; Rusin, Kochanek, & Keeton 2003), and the formation and evolution of galaxies (Kochanek et al. 2000; Kochanek & White 2001; Keeton 2001a; Oguri 2002; Ofek, Rix, & Maoz 2003). A large homogeneous sample of lensed quasars with a well-understood selection function is essential in these statistical studies. In addition, lensed

quasars can be a powerful tool to study quasar itself through microlensing, spectra, or variabilities of lensed quasars (Chang & Refsdal 1984; Grieger, Kayser, & Schramm 1991; Mediavilla et al. 1998; Mineshige & Yonehara 1999; Yonehara 1999; Wyithe, Webster, & Turner 2000; Yonehara 2001; Lewis & Ibata 2003). Therefore, it is important to make a large sample of lensed quasars also to find more gravitational lens systems which are suitable for studying quasar.

The Sloan Digital Sky Survey (SDSS; York et al. 2000; Stoughton et al. 2002; Abazajian et al. 2003) has the potential to provide such a lensed quasar sample. The SDSS is a survey to image 10^4deg^2 of the sky as well as to obtain spectra of galaxies and quasars from the imaging data. The dedicated 2.5 meter telescope at Apache Point Observatory is equipped with a multi-CCD camera (Gunn et al. 1998) with five broad band centered at 3561, 4676, 6176, 7494, and 8873 Å (Fukugita et al. 1996). The

imaging data are automatically reduced by the photometric pipeline (Lupton et al. 2001). The astrometric positions are accurate to about $0''.1$ for sources brighter than $r = 20.5$ (Pier et al. 2003). The photometric errors are typically less than 0.03 magnitude (Hogg et al. 2001; Smith et al. 2002). The SDSS quasar selection algorithm is presented in Richards et al. (2002); the SDSS spectra cover 3800–9200 Å at a resolution of 1800–2100. The final spectroscopic quasar sample is expected to comprise 10^5 quasars, thus will contain $\sim 10^2$ lensed quasars given the typical lensing probability 0.1% (Turner, Ostriker, & Gott 1984). Indeed, several new gravitational lens systems have been discovered using SDSS data (Inada et al. 2003a,b,2004; Morgan, Snyder, & Reens 2003; Johnston et al. 2003; Pindor et al. 2004; Oguri et al. 2004).

We report the discovery of the lensed quasar SDSS J133534.79+011805.5 (SDSS J1335+0118) in the SDSS. This quasar has already been identified in the Large Bright Quasar Survey (LBQS 1333+0133; Hewett et al. 1991), but not as lensed. A search for lens candidates in the LBQS was carried out by Hewett et al. (1998), but those authors state that their search is not sensitive to lens systems with $\leq 3''$ separations. The quasar was selected as a lens candidate in the course of an ongoing search for strongly lensed quasars in the SDSS. From the results of photometric and spectroscopic follow-up observations, we conclude that the quasar is lensed by an intervening galaxy.

2. Observations

2.1. Candidate Selection

To select SDSS lensed quasar candidates, we examine all spectroscopically confirmed quasars with $z > 0.6$. Quasars at smaller redshifts have much lower probability of being lensed and also are often extended because of their host galaxies, making it more difficult to select lens candidates with our candidate selection algorithm described below. We search for lens candidates using a combination of SDSS parameters: `dev_L` (the likelihood parameter of fitting by de Vaucouleurs profile), `exp_L` (the likelihood parameter of fitting by exponential disk), and `star_L` (the likelihood parameter of fitting by point spread function). This candidate selection algorithm has already found three new lensed quasar systems (Inada et al. 2003a,2004; Pindor et al. 2004), and can identify gravitationally lensed quasars with image separations $1''.0 - 2''.5$ quite well (N. Inada et al., in preparation). The SDSS *ugriz* imaging data of SDSS J1335+0118 (see Figure 1) clearly shows that the system consists of two stellar components with similar colors, making it an excellent lensing candidate. The total magnitudes of this system in the SDSS photometric data are $u = 18.21 \pm 0.02$, $g = 17.83 \pm 0.01$, $r = 17.62 \pm 0.01$, $i = 17.26 \pm 0.01$, and $z = 17.14 \pm 0.03$.

2.2. Additional Imaging Observations

We obtained a deep *i*-band image on 2003 May 28 with the Subaru Prime Focus Camera (Suprime-Cam; Miyazaki et al. 2002) of the National Astronomical Observatory of

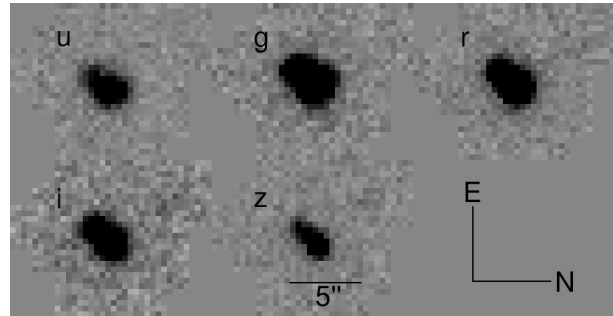


Fig. 1. SDSS images of SDSS J1335+0118 in all bands. The image scale is $0''.396\text{pixel}^{-1}$.

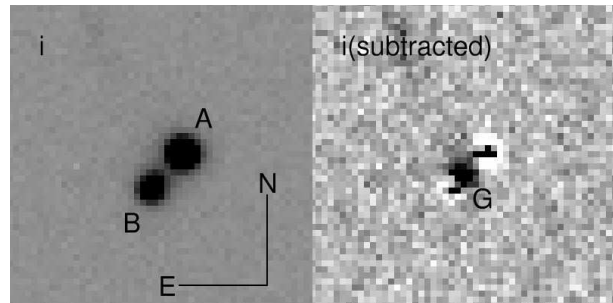


Fig. 2. Subaru Suprime-cam images of SDSS J1335+0118 in the *i*-band. The image scale is $0''.2\text{pixel}^{-1}$. *Left:* original Suprime-cam image. Components A and B are lensed quasar components. *Right:* PSF-subtracted image. The component G is likely to be the lens galaxy.

Japan's Subaru 8.2-m telescope, which is shown in Figure 2. The exposure time was 30 seconds and the seeing was $0''.5 - 0''.6$. The image scale is $0''.2\text{pixel}^{-1}$. Each frame was bias-subtracted and flat-field corrected. Subtraction of the two quasar images using a nearby star as a point-spread function (PSF) template reveals an extended object, denoted as G, located on the line between A and B and closer to B (see Figure 2). This configuration is expected for a standard simple lens model such as singular isothermal sphere model, so component G is likely to be the lens galaxy. In Table 1, we summarize the position of each component and the relative fluxes of the quasar components that are measured using Subaru Suprime-cam data. The errors of the galaxy position is determined from Gaussian fits.

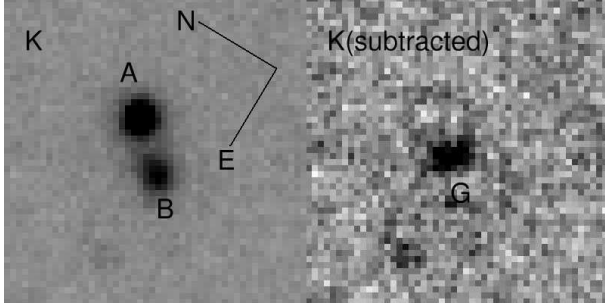
We also obtained *J* and *K*-band data on 2003 April 19 with the Near InfraRed Camera (NIRC; Matthews & Soifer 1994) of the Keck I telescope at the W. M. Keck Observatory on Mauna Kea, Hawaii, USA. The total exposure time was 900 seconds, seeing was variable, averaging $\sim 0''.6$. Conditions were not photometric, with about 1 magnitude of variable cloud. The image scale is $0''.15\text{pixel}^{-1}$. Standard reduction procedures were followed to remove the dark current and to flat field the data. We show the *K* image in Figure 3. Although the galaxy component can be seen in the direct image, we subtracted the PSF of two quasar components by fitting a Gaussian

Table 1. Positions and flux ratios of SDSS J1335+0118 in the Subaru *i*-band image

Object	$x[\text{arcsec}]^*$	$y[\text{arcsec}]^*$	Flux[arbitrary] [†]
A	0.000 ± 0.001	0.000 ± 0.001	1.0 ± 0.2
B	-1.038 ± 0.002	-1.165 ± 0.002	0.374 ± 0.075
G	-0.769 ± 0.011	-0.757 ± 0.011	...

* The positive directions of x and y are defined by West and North, respectively.

† Errors are broadened to 20% to account for possible systematic effects.

**Fig. 3.** Same as Figure 2, but the *K*-band images taken with NIRC on Keck I telescope are shown. The image scale is $0''.15\text{pixel}^{-1}$.

PSF at each quasar location, revealing the lensing galaxy more clearly (see Figure 3). As in the *i*-band image shown in Figure 2, the galaxy component is seen in the PSF-subtracted *K*-band image. We compare the distance between components A, B, and G in Table 2. The differences of the distances are large, but only $\sim 0''.1$ at most and still much smaller than seeing sizes and pixel sizes. The position of the lens galaxy is particularly uncertain in the *K* data because not only is the lensing galaxy relatively faint and extended, but also because the seeing was quite variable on the night the IR data were obtained and no suitable PSF star is present in the NIRC field, making it difficult to properly subtract the PSF wings which overlap the galaxy. Thus it may be possible that such residuals systematically affect the estimated positions. We note that the system is detected (but not resolved) by the Two-Micron All-Sky Survey (2MASS) with $J = 16.23 \pm 0.10$, $H = 15.47 \pm 0.11$, and $K = 15.29 \pm 0.18$.

2.3. Spectroscopic Observations

The spectroscopic observation was done on 2003 March 2 with the red CCD of the ESO Multi-Mode Instrument (EMMI) on the ESO New Technology Telescope (NTT). We used grism #3 (360 line mm^{-1} , $2.3\text{ \AA pixel}^{-1}$, covering $3850 - 8450\text{ \AA}$). The seeing was $1''.0$. The exposure time was 900 sec. The slit was positioned to obtain spectra of the two quasar components (A and B) simultaneously. The two components were clearly separated in the EMMI image, making extraction simple. The data were reduced in a standard way using IRAF¹. The spectra are

shown in Figure 4. We find that both components A and B have C IV, C III], and Mg II emission lines at the same wavelengths. The redshifts of components A and B estimated from Mg II emission lines are $z = 1.57 \pm 0.03$ and $z = 1.57 \pm 0.05$, respectively. We cross-correlate the two spectra and estimate the velocity difference between two quasar components to be $20 \pm 800\text{ km s}^{-1}$. We also plot the ratio of the fluxes of components A and B, and find that the ratio is almost constant (~ 0.35) for a wide range of wavelengths. Therefore we conclude that components A and B are two gravitationally lensed images of a quasar at $z = 1.57$. The lens hypothesis is further supported by the fact that both components appear to have associated C IV absorption at a blueshift of 2500 km s^{-1} from the quasar. We note that both A and B have strong Fe II/Mg II/Mg I absorption system at $z = 1.43$, Al II absorption system at $z = 1.42$. This absorption is unlikely to be associated with the lens, given the small difference between the absorption and source redshifts. Indeed, the lensing galaxy is typically half way out in affine or angular diameter distance, and probabilities of such small difference between source and lens redshifts are too small (e.g., Ofek, Rix, & Maoz 2003). Moreover, such absorption is quite common since the typical linear separation between quasar sightlines and galaxies which are responsible for such absorption is large, $\sim 50\text{ kpc}$ (Bergeron & Boisse 1991; Fukugita, Hogan, & Peebles 1996). It seems that strengths of absorptions are different between components A and B, but this is not surprising given the inhomogeneity of the spatial distribution of absorbers (e.g., Petitjean & Bergeron 1990; Steidel & Sargent 1992). We note that the color of component G (see §2.4) is consistent with that of a low-redshift ($z \lesssim 0.5$) early-type galaxy (e.g., McLeod et al. 1995).

2.4. Differential Extinction

We check colors of quasar components to see whether the system suffer from differential extinction. The results of photometry from the imaging data of the SDSS, Subaru, and Keck are shown in Table 3. Relative magnitudes are estimated from Subaru, Keck, and SDSS images. To calibrate total magnitudes, we use the measurements of the SDSS, $i = 17.26 \pm 0.01$, and the 2MASS, $K = 15.29 \pm 0.18$. We find that the colors of each component are consistent with a single value, given the errors of $\sim 0.1\text{ mag}$ associated with the deconvolution of two components. Spectra of quasar components shown in Figure 4 also indicates no significant differential extinction. Although it seems that at $\lesssim 4800\text{ \AA}$ the ratio increases as the wavelength de-

¹ IRAF is distributed by the National Optical Astronomy Observatories, which are operated by the Association of Universities for Research in Astronomy, Inc., under cooperative agreement with the National Science Foundation.

Table 2. Comparison of positions between Subaru *i*-band and Keck *K*-band images

Objects	<i>i</i> -band Distance[arcsec]	<i>K</i> -band Distance[arcsec]
AB	1.560 ± 0.002	1.503 ± 0.002
AG	1.079 ± 0.011	0.969 ± 0.012
BG	0.489 ± 0.011	0.542 ± 0.012

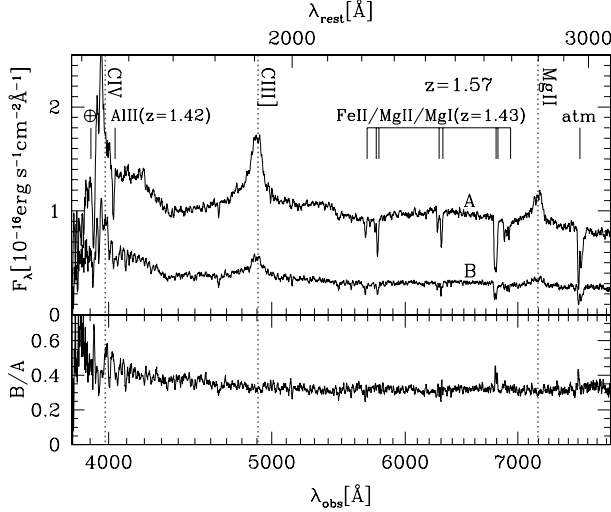


Fig. 4. ESO NTT spectra of SDSS J1335+0118 components A and B. The redshifts of components A and B estimated from Mg II emission lines are $z = 1.57 \pm 0.03$ and $z = 1.57 \pm 0.05$, respectively. Both components have associated C IV absorption at a blueshift of 2500 km s^{-1} from the quasar (marked by \oplus). In addition, both components have strong Fe II/Mg II/Mg I absorption system at $z = 1.43$, and Al II absorption system at $z = 1.42$. Note that the absorption at $\sim 7600 \text{ \AA}$ is atmospheric. The bottom panel shows the ratio of spectra.

creases, but the feature is not significant because of the large errors in those wavelengths arising from the low response at $\sim 4000 \text{ \AA}$ or shorter. Therefore we conclude that differential reddening is not significant.

3. Mass Modeling

We model the lens system with the simple Singular Isothermal Ellipsoid (SIE) model, assuming that component G is the lens galaxy. The SIE model has the following dimensionless surface mass density:

$$\kappa(r) = \frac{r_{\text{ein}}}{2\zeta}, \quad (1)$$

where $\zeta = r[1 + ((1 - q^2)/(1 + q^2)) \cos 2(\theta - \theta_e)]^{1/2}$, r_{ein} is the Einstein ring radius, q is the lens axis ratio, and θ_e is the position angle of the ellipse. The model includes eight parameters: the galaxy position x_g and y_g , the Einstein ring radius r_{ein} , the ellipticity $e = 1 - q$, the position angle θ_e , the source position x_s and y_s , and the flux of the quasar f^2 . Since the number of constraints is also eight

² We obtain the same results even if we do not adopt a parameter f and instead we use only the flux ratio, not fluxes of A and B, as a constraint.

Table 4. Best fit SIE model parameters for SDSS J1335+0118

Parameter	Value
$r_{\text{ein}}[\text{arcsec}]$	$0.789^{+0.009}_{-0.011}$
e	$0.123^{+0.041}_{-0.024}$
$\theta_e[\text{deg}]$	$-7.8^{+19.3}_{-12.0}$

We use positions and flux ratios of SDSS J1335+0118 in the Subaru *i*-band image (see Table 1). Errors are 68% confidence.

(see Table 1), the degree of freedom is zero. We use the public software *lensmodel* (Keeton 2001b) to constrain the models. The result is summarized in Table 4. The best-fit parameters predict the time delay between images as $\Delta t = 29.5 h^{-1} \text{ day}$ (h denotes the Hubble constant in units of $100 \text{ km s}^{-1} \text{ Mpc}^{-1}$) if we adopt a lens redshift 0.5, $\Omega_M = 0.3$, and $\Omega_\Lambda = 0.7$. Errors on the parameters are estimated from one-dimensional slices of the χ^2 surface. We find that we can fit the lens system with relatively small lens ellipticity $e = 0.123^{+0.041}_{-0.024}$, significantly smaller than observed ellipticity of the light (~ 0.3). The derived position angle of the lens galaxy is consistent with that of the light ($\sim 7^\circ$) within 1σ . These results are in good agreement with previous studies (e.g., Keeton, Kochanek, & Falco 1998).

4. Conclusion

We have reported the discovery of a new two-image gravitational lens SDSS J1335+0118. The system was identified as a new lens candidate in the SDSS. The image separation is $1''.56 \pm 0.002$ in the *i*-band image taken with Subaru Suprime-cam. The spectroscopic observation with ESO NTT has confirmed both images have identical redshift $z = 1.57$ ($z = 1.57 \pm 0.03$ and $z = 1.57 \pm 0.05$ for components A and B, respectively). We have also probably identified the lensing galaxy between two quasar components in the higher-resolution imaging data taken with Subaru Suprime-cam and Keck NIRC. The lens geometry is well reproduced with a simple mass model and reasonable model parameters. Assuming the redshift of the lens galaxy as 0.5, we have predicted a differential time delay $\Delta t \sim 30 h^{-1} \text{ day}$.

We thank an anonymous referee for many useful comments. Funding for the creation and distribution of the SDSS Archive has been provided by the Alfred P. Sloan Foundation, the Participating Institutions, the National Aeronautics and Space Administration, the National

Table 3. Photometry of Subaru *i*-band, Keck *K*-band, and SDSS *ugriz*-band images

Band	Total	A	B	B–A	G
<i>u</i> (SDSS)	$18.21 \pm 0.02^*$	18.54	19.68	1.14	...
<i>g</i> (SDSS)	$17.83 \pm 0.01^*$	18.12	19.39	1.27	...
<i>r</i> (SDSS)	$17.62 \pm 0.01^*$	17.95	19.09	1.14	...
<i>i</i> (SDSS)	$17.26 \pm 0.01^*$	17.60	18.68	1.08	...
<i>i</i> (Subaru)	$17.26 \pm 0.01^*$	17.63	18.70	1.07	20.05
<i>z</i> (SDSS)	$17.14 \pm 0.03^*$	17.49	18.54	1.05	...
<i>K</i> (Keck)	$15.29 \pm 0.18^\dagger$	15.78	16.75	0.97	17.81

* Based on the SDSS.

† Based on the 2MASS.

Science Foundation, the U.S. Department of Energy, the Japanese Monbukagakusho, and the Max Planck Society. The SDSS Web site is <http://www.sdss.org/>.

The SDSS is managed by the Astrophysical Research Consortium (ARC) for the Participating Institutions. The Participating Institutions are The University of Chicago, Fermilab, the Institute for Advanced Study, the Japan Participation Group, The Johns Hopkins University, Los Alamos National Laboratory, the Max-Planck-Institute for Astronomy (MPIA), the Max-Planck-Institute for Astrophysics (MPA), New Mexico State University, University of Pittsburgh, Princeton University, the United States Naval Observatory, and the University of Washington.

Part of the work reported here was done at the Institute of Geophysics and Planetary Physics, under the auspices of the U.S. Department of Energy by Lawrence Livermore National Laboratory under contract No. W-7405-Eng-48.

This work is based in part on data collected at Subaru Telescope, which is operated by the National Astronomical Observatory of Japan, and partly based on observations collected at the European Southern Observatory, Chile under program 70.D-0469. Some of the Data presented herein were obtained at the W.M. Keck Observatory, which is operated as a scientific partnership among the California Institute of Technology, the University of California and the National Aeronautics and Space Administration. The Observatory was made possible by the generous financial support of the W.M. Keck Foundation. The authors wish to recognize and acknowledge the very significant cultural role and reverence that the summit of Mauna Kea has always had within the indigenous Hawaiian community. We are most fortunate to have the opportunity to conduct observations from this mountain. We thank the staffs of Subaru, Keck, and ESO NTT for their excellent assistance.

References

Abazajian, K., et al. 2003, *AJ*, 126, 2081
 Bergeron, J., & Boisse, P. 1991, *A&A*, 243, 344
 Chae, K.-H., et al. 2002, *Phys. Rev. Lett.*, 89, 151301
 Chang, K., & Refsdal, S. 1984, *A&A*, 132, 168
 Chiba, M. 2002, *ApJ*, 565, 17
 Dalal, N., & Kochanek, C. S. 2002, *ApJ*, 572, 25
 Fukugita, M., Futamase, T., & Kasai, M. 1990, *MNRAS*, 246,

24P
 Fukugita, M., Hogan, C. J., & Peebles, P. J. E. 1996, *Nature*, 381, 489
 Fukugita, M., Ichikawa, T., Gunn, J. E., Doi, M., Shimasaku, K., & Schneider, D. P. 1996, *AJ*, 111, 1748
 Grieger, B., Kayser, R., & Schramm, T. 1991, *A&A*, 252, 508
 Gunn, J. E., et al. 1998, *AJ*, 116, 3040
 Hewett, P. C., Foltz, C. B., Chaffee, F. H., Francis, P. J., Weymann, R. J., Morris, S. L., Anderson, S. F., & MacAlpine, G. M. 1991, *AJ*, 101, 1121
 Hewett, P. C., Foltz, C. B., Harding, M. E., & Lewis, G. F. 1998, *AJ*, 115, 383
 Hogg, D. W., Finkbeiner, D. P., Schlegel, D. J., & Gunn, J. E. 2001, *AJ*, 122, 2129
 Inada, N., et al. 2003a, *AJ*, 126, 666
 Inada, N., et al. 2003b, *Nature*, 426, 810
 Inada, N., et al. 2004, *AJ*, submitted
 Johnston, D. E., et al. 2003, *AJ*, 126, 2281
 Keeton, C. R. 2001a, *ApJ*, 561, 46
 Keeton, C. R. 2001b, preprint (astro-ph/0102340)
 Keeton, C. R., Kochanek, C. S., & Falco, E. E. 1998, *ApJ*, 509, 561
 Kochanek, C. S. 1991, *ApJ*, 373, 354
 Kochanek, C. S., & White, M. 2001, *ApJ*, 559, 531
 Kochanek, C. S., et al. 2000, *ApJ*, 543, 131
 Koopmans, L. V. E., & Treu, T. 2003, *ApJ*, 583, 606
 Lewis, G. F., & Ibata, R. A. 2003, *MNRAS*, 340, 562
 Lupton, R., Gunn, J. E., Ivezić, Z., Knapp, G. R., Kent, S., and Yasuda, N. 2001, in ASP Conf. Ser. 238, *Astronomical Data Analysis Software and Systems X*, ed. F. R. Harnden, Jr., F. A. Primini, and H. E. Payne (San Francisco: Astr. Soc. Pac.), p. 269 (astro-ph/0101420)
 Matthews, K., & Soifer, B. T. 1994, *ASSL Vol. 190: Astronomy with Arrays, The Next Generation*, 239
 Mediavilla, E., et al. 1998, *ApJL*, 503, L27
 Metcalf, R. B., & Madau, P. 2001, *ApJ*, 563, 9
 Mineshige, S., & Yonehara, A. 1999, *PASJ*, 51, 497
 McLeod, B. A., Bernstein, G. M., Rieke, M. J., Tollestrup, E. V., & Fazio, G. G. 1995, *ApJS*, 96, 117
 Miyazaki, S., et al. 2002, *PASJ*, 54, 833
 Morgan, N. D., Snyder, J. A., & Reens, L. H. 2003, *AJ*, 126, 2145
 Oguri, M. 2002, *ApJ*, 580, 2
 Oguri, M., et al. 2004, *ApJ*, in press (astro-ph/0312429)
 Ofek, E. O., Rix, H., & Maoz, D. 2003, *MNRAS*, 343, 639
 Pier, J. R., Munn, J. A., Hindsley, R. B., Hennessy, G. S., Kent, S. M., Lupton, R. H., & Ivezić, Ž. 2003, *AJ*, 125, 1559
 Petitjean, P., & Bergeron, J. 1990, *A&A*, 231, 309
 Pindor, B., et al. 2004, *AJ*, in press (astro-ph/0312176)

- Refsdal, S. 1964, MNRAS, 128, 307
Refsdal, S. 1966, MNRAS, 132, 101
Richards, G. T., et al. 2002, AJ, 123, 2945
Rusin, D., Kochanek, C. S., & Keeton, C. R. 2003, ApJ, 595, 29
Schechter, P. L., Wambsganss, J. 2002, ApJ, 580, 685
Schmidt, M., Schneider, D. P., & Gunn, J. E. 1995, AJ, 110, 68
Smith, J. A., et al. 2002, AJ, 123, 2121
Steidel, C. C., & Sargent, W. L. W. 1992, ApJS, 80, 1
Stoughton, C., et al. 2002, AJ, 123, 485
Turner, E. L. 1990, ApJL, 365, L43
Turner, E. L., Ostriker, J. P., & Gott, J. R. 1984, ApJ, 284, 1
Wambsganss, J., & Paczynski, B. 1991, AJ, 102, 864
Wyithe, J. S. B., Webster, R. L., & Turner, E. L. 2000, MNRAS, 318, 762
Yonehara, A. 1999, ApJL, 519, L31
Yonehara, A. 2001, ApJL, 548, L127
York, D. G., et al. 2000, AJ, 120, 1579